



Sharpness improvement of surgical blade by means of ZrCuAlAgSi metallic glass and metallic glass thin film coating

P.H. Tsai^a, Y.Z. Lin^b, J.B. Li^b, S.R. Jian^a, J.S.C. Jang^{b,c,*}, C. Li^b, J.P. Chu^d, J.C. Huang^e

^a Department of Materials Science and Engineering, I-Shou University, Kaohsiung 840, Taiwan

^b Department of Mechanical Engineering, National Central University, Chung-Li 32001, Taiwan

^c Institute of Material Science and Engineering, National Central University, Chung-Li 32001, Taiwan

^d Department of Materials Science and Engineering, National Taiwan University of Science and Technology, Taipei 10607, Taiwan

^e Department of Materials and Optoelectronic Science, Center for Nanoscience and Nanotechnology, National Sun Yat-Sen University, Kaohsiung 804, Taiwan

ARTICLE INFO

Article history:

Received 20 April 2012

Received in revised form

29 May 2012

Accepted 26 June 2012

Available online 20 July 2012

Keywords:

B. Glasses, metallic

C. Casting

C. Thin films

F. Mechanical testing

G. Biomedical applications

ABSTRACT

Zr-based bulk metallic glasses (BMGs) possess excellent unique properties, such as high mechanical properties, good corrosion resistance, long-term antimicrobial ability, and were considered as an ideal candidate for medical tools. In this study, self-made ZrCuAlAgSi BMG surgical blade and commercial martensitic steel blade with and without metallic glass thin film (MGTF) were carefully examined for their sharpness. The amorphous state of BMG and MGTF were ascertained by X-ray diffraction (XRD) and differential scanning calorimetry (DSC) analysis. A specially designed indentation-cutting rig was established to evaluate the sharpness of each blade on cutting the soft rubber material. The sharpness was evaluated by the blade sharpness index (BSI) which represents the ratio of external work done by the load to the energy required to initiate a cut or crack inside given materials. Results of sharpness test reveal that both BMG blade and the MGTF coated blade exhibits much lower surface roughness at their tip-edge and smaller BSI values (0.25 and 0.23, respectively) than the commercial blade (~ 0.34), which corresponds to 26.5% and 32% improvement on the sharpness, respectively.

© 2012 Elsevier Ltd. All rights reserved.

1. Introduction

In the past few decades, Zr-based bulk metallic glasses (BMGs) have attracted lots of attention owing to its good engineering properties such as high glass forming ability (GFA), high yield strength and elastic strain, good thermal stability and great corrosion resistance [1–8]. In parallel, Zr-based BMGs possess a wide range of super-cooled liquid phase about 100 K, which allows them to be processed into complex-shaped components by thermoplastic forming [9,10]. The combined quality in their mechanical and chemical properties gives great advantages for Zr-based BMGs to be an excellent choice for medical implants, surgical tools and other biomedical related components [11–17].

Of all materials for surgical tools, martensitic stainless steel is the most common one, especially in surgical blades. The polycrystalline structures in martensitic stainless steels consist of

large number of grains with their average sizes about 10 microns. This implies that the presence of numerous grain boundaries can serve as centers for the initiation of cracks and fracture when blades underwent grinding. The argument was attested by the observation of irregular, wavy surfaces at the magnified (1000 \times) edge-tip of surgical blades in [3]. When such a surgical blade is used to cut soft tissues, fragmental surfaces of wound tissues by tearing and snatching were easily created and hence more difficult to be sutured and recovered. This is one issue that BMGs can be a substitution for conventional stainless steels by the advantages of their amorphous microstructures. Similar idea can be utilized if a metallic glass thin film (MGTF) is coated on stainless steels instead of bulk BMGs. The coating can be routinely fabricated by a DC magnetron sputtering. The MGTF usually has smaller surface roughness down to 5 nm or lower, which can help preventing bacterial attachment, reducing the friction and improving the sharpness of blades [12,16].

The sharpness of a blade at its edge-tip is important when evaluating its efficiency in slicing, cutting and chopping. The sharpness mainly depends on the geometry of the blades and properties of working target as well [17]. High sharpness means

* Corresponding author. Department of Mechanical Engineering, National Central University, Chung-Li 32001, Taiwan. Tel.: +886 3 4267379; fax: +886 3 4254501.
E-mail address: jscjang@ncu.edu.tw (J.S.C. Jang).

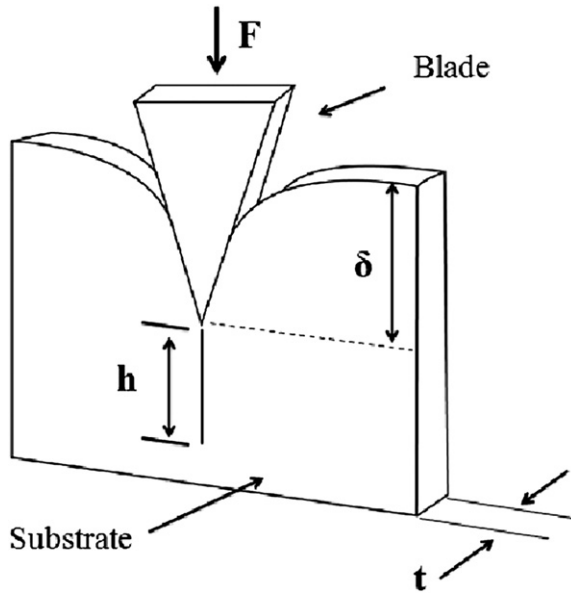


Fig. 1. An idealization of the indentation type cutting process.

faster and cleaner cut, which leads to less pain, better healing and less scarring of the wound [18,19]. The sharpness can be evaluated in a way similar to the principle in fracture mechanics that certain critical energy is required to initiate a crack in materials with given geometry and mechanical properties. Following this concept, the “blade sharpness index” (BSI) was proposed to evaluate the sharpness of cutter as reported by McCarthy [20,21]. This quantitative measure is defined as

$$BSI = \frac{\int_0^{\delta_i} F dx}{\delta_i t J_{IC}} \quad (1)$$

and illustrated in Fig. 1 where F is applied force, dx is increment of blade displacement, δ_i is initial depth of blade indentation before substrate fracture, h is length of cut surface, t is thickness of substrate material, J_{IC} is model I fracture toughness of the substrate

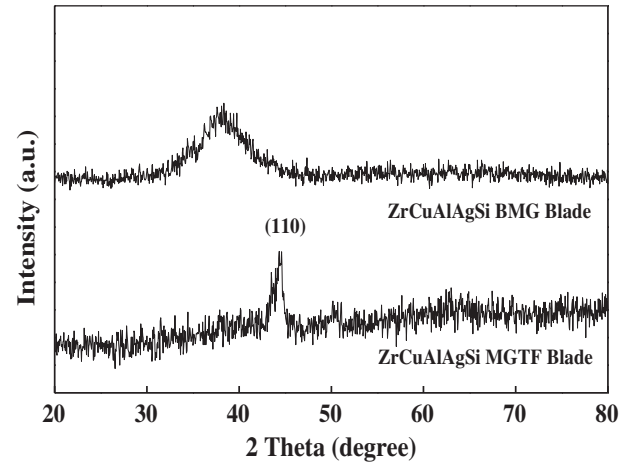


Fig. 3. XRD results of ZrCuAlAgSi BMG blade and ZrCuAlAgSi MGTF coated blade.

or referred as the resistance to fracture. Physically, Eq. (1) is a ratio of external work done by the load to the energy required to initiate a cut or crack of area $\delta_i t$ inside material with fracture toughness J_{IC} . It also implies that the blade sharpness is proportional inversely to δ_i , the indentation depth to initiate a cut or crack in the substrate. Typical BSI varies between 0.2 for sharp blade and 0.5 for blunt one.

In this study, three surgical blades including a commercial one, a commercial one with ZrCuAlAgSi MGTF, and self-made ZrCuAlAgSi BMG were prepared and investigated for their microstructures, edge-tip surface morphologies, the cutting process and sharpness evaluation following the work proposed by McCarthy.

2. Experimental procedure

The pre-alloyed ingots of $Zr_{48}Cu_{35.3}Al_8Ag_8Si_{0.7}$ (ZrCuAlAgSi) were prepared by arc melting. All elements of pure Zr, Cu, Al, Ag, and Si were carefully measured and melted by arc-melting under a Ti-gettered argon atmosphere. The ingots were re-melted four times in a furnace with purified argon atmosphere to ensure their homogeneity. In the last melting, the liquid alloy was suction cast into a water-cooling Cu mold to form plates

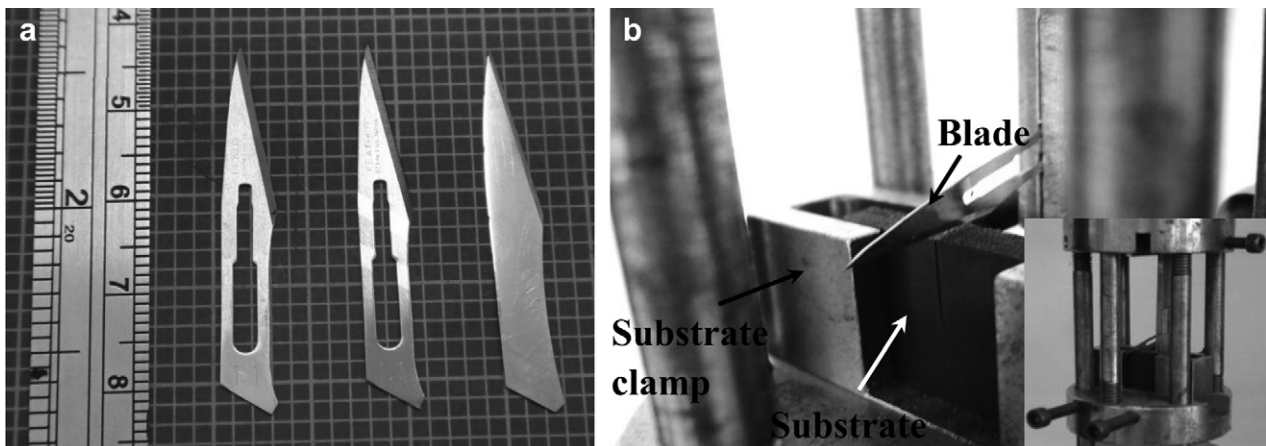


Fig. 2. (a) Three blades studied in this research: commercial blade, ZrCuAlAgSi MGTF coated blade, and ZrCuAlAgSi BMG blade (left to right). (b) Experimental rig used for indentation-cutting test; insert is the whole set rig.

with dimension of 30 mm W × 80 mm L × 2 mm T and 3 mm T, respectively. The BMG plates with 2 mm thickness were machined into a shape of scalpel blade by wire electrical discharge cutting (EDC) process. The blade was then reduced in thickness, sharpened at its edge-tip and finally fine polished. The edge-tip has angle of 30° identical to the commercial blade. The other 3 mm thick BMG plates were lathed and assembled into discs with 2-in diameter used as the target for sputtering.

For the MGTF, a 200 nm-thick ZrCuAlAgSi film and 50 nm Ti thin film buffer layer were coated onto commercial blades (No.11, FEATHER Safety Razor Co.) by DC sputtering system (MDX1000). The operating conditions of DC sputtering system were set as follows: the base pressure of 6×10^{-6} torr, working pressure at 4 mtorr, Ar flow of 5.4 sccm, sputtering time of 30 min and 30 W sputtering powers.

Fig. 2(a) shows all three blades used in this study. The amorphous state of BMG plates and MGTF was ascertained by x-ray diffraction analysis (XRD, Scintag X-400 X-ray diffractometer for BMG, Bruker D8 Discover Diffractometer-incident beam for MGTF) with monochromatic Cu-K α radiation. The surface morphology of blade edge-tip was examined by scanning electron microscopy (SEM, Hitachi S4700 FESEM) with energy dispersive spectrum capability (EDS). The adhesion was detected by the J&L Tech Scratch Tester with a 200 μ m-sized diamond probe. The initial load is set to 0.2 N and the maximum load is 100 N under indent speed of 0.08 mm/s.

A specially designed rig is shown in Fig. 2(b) to measure the blade sharpness during cutting. The rig was connected to a 50 kN Hung-Da universal testing machine. The blade was fixed into the upper holder with an angle of 45° then cuts through a rubber (styrene-butadiene rubber, SBR) at a speed of 9 mm/min.

The dimension of rubber is 5 mm thick and 10 mm high. The experiment was conducted in two turns. The first cut is to register the load-indentation (displacement) curve. The second pass is to move the blade down along the cut and record load and indentation (displacement) another time. The second pass is meant to measure the total friction force between the blade and substrate.

3. Results and discussion

The as-cast ZrCuAlAgSi BMG plates were examined by XRD and EDS to confirm their amorphous state and compositions. EDS analysis reveals that the composition of ZrCuAlAgSi BMG plate and the target are very close to each other with only 0.25 at% difference.

Fig. 3 shows the XRD pattern of the final BMG blades where a broad peak between 30 and 50° confirms the ZrCuAlAgSi retain its amorphousness even after EDC and polishing. Fig. 3 also shows the XRD pattern of MGTF coated blade where only one peak at $2\theta = 44.7^\circ$ can be clearly identified corresponding to the phase of crystalline iron. Note the MGTF is only 200 nm thick that makes the incident beam XRD difficult to detect the film's microstructure.

The surface morphology of blade edge-tip was examined by SEM at the location of blade edge where marked with dashed circle as shown in Fig. 4(d). Fig. 4(a)–(c) shows the surface morphology of edge-tip of commercial blade, BMG blade and MGTF coated blade, respectively. Both the BMG and MGTF coated blade have their finished surface very smooth except few sparse scratches. This is a comparison to the commercial one which surface has significant irregular grooves. The highly smooth surface after finishing implies that less friction forces during

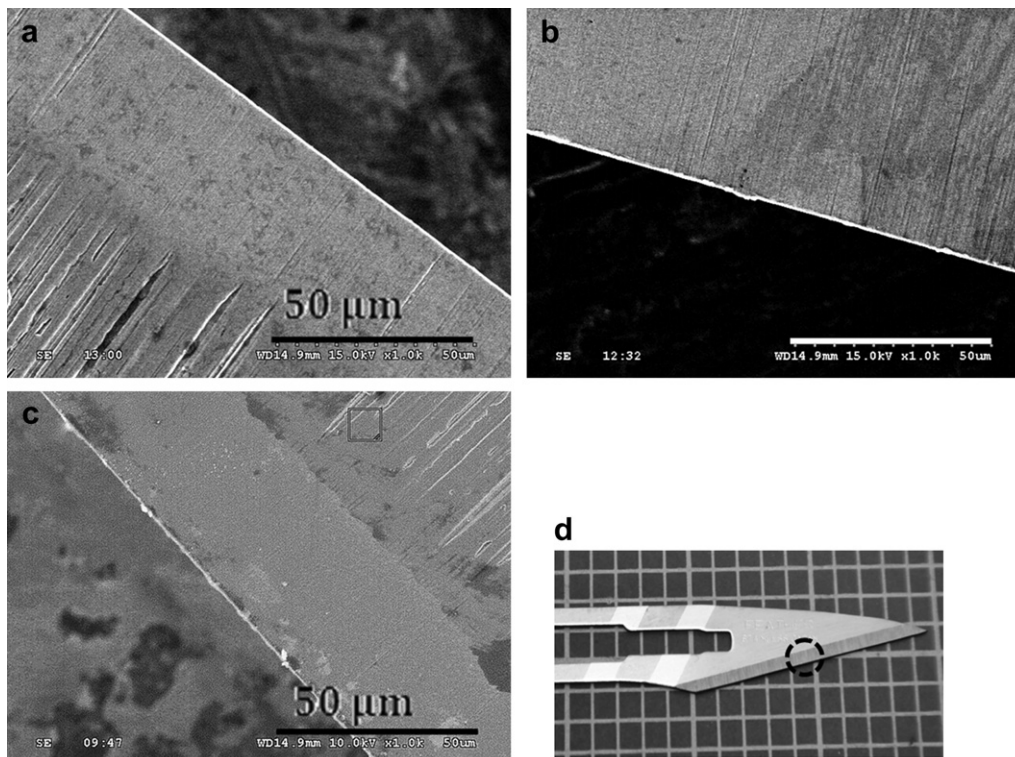


Fig. 4. SEM images of blade edge-tip; (a) commercial blade; (b) ZrCuAlAgSi BMG blade, (c) ZrCuAlAgSi MGTF coated blade. (d) Mark of dashed circle on the blade edge indicates the location of SEM observation.

cutting. The surface profiles scanned by SEM in Fig. 5 further confirm the observations in Fig. 4 that the roughness of commercial blade is $\sim 1.2 \mu\text{m}$ on average and can be significantly reduced to $\sim 0.3 \mu\text{m}$ in the BMG blade and $\sim 0.2 \mu\text{m}$ in the MGTF coated blade.

Scratch tests were also carried out for testing the bonding strength between MGTF and substrate. A diamond tip was applied on the surface of MGTF blade with increased loading till the film was ruptured. The detached load was found to be around 60 N as shown in Fig. 6. This indicates the adhesion between MGTF and martensitic steel substrate is comparable to the level of industrial requirement.

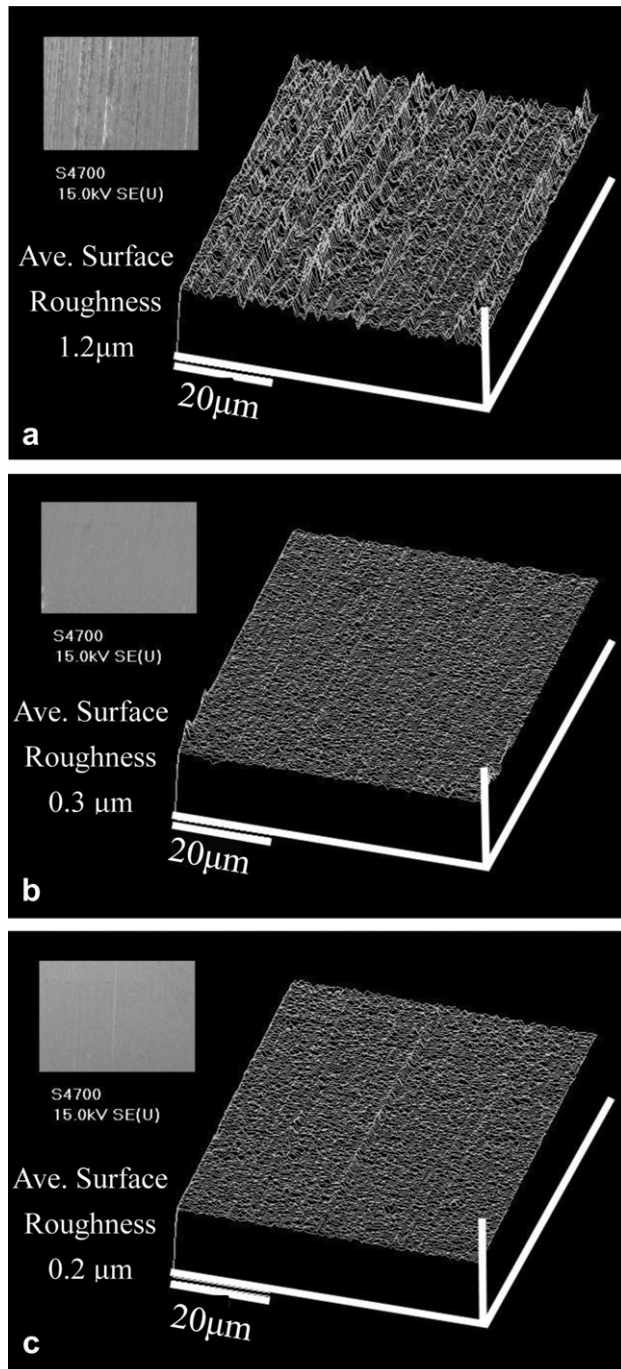


Fig. 5. Images of SEM scanning surface profile of blade edge; (a) commercial blade, (b) ZrCuAlAgSi BMG blade, and (c) ZrCuAlAgSi MGTF coated blade.

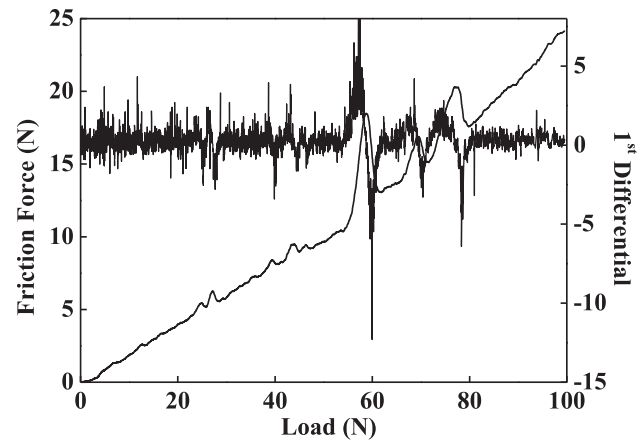


Fig. 6. Profile of friction force as a function of applied loading during scratch test for ZrCuAlAgSi MGTF coated blade.

Fig. 7(a) shows the load–displacement curves under first cut for all three blades by indentation–cutting experiment. Similar behaviors were found. All have linear relation between the loading and displacement at first until around 2 mm, representing the process of indentation. Then nonlinear curves started to develop with lower slope as the cutting through the substrate. The slope of curves in Fig. 7(a) gives the stiffness–displacement relation in Fig. 7(b). The maximum of this curve defines the value of δ_i – the initial indentation right before fracture. The commercial blade has the highest δ_i among all, which indicates a larger resistance from the substrate during cutting.

The second pass (free pass) was carried out after the first cutting pass. This gives another load–displacement curve as shown in Fig. 8(a) for the MGTF coated blade. A linear curve (P) represents the proportional relation between load and displacement which comes from the frictional force between blade and substrate.

In view of Eq. (1), there are other quantities required to give the numerical values of BSI. First, the area underneath the load–displacement curve ($\int_0^{\delta_i} F dx$) represents the work done by external load before substrate fractured. The initiation fracture toughness J_{Ic} can be obtained as follow:

$$J_{Ic} = \frac{(X - P)u}{dA} \quad (2)$$

where X is the force acting on the blade, P is the total friction force acting between the blade and substrate, u is the blade displacement, and dA is an increment of newly created surface area due to cutting which is equal to $2ht$ as illustrated in Fig. 1. The interaction strength ($X - P$) between blade and substrate were recorded in each step during test. Fig. 8(b) demonstrates a constant toughness J_{Ic} as cutting moves into the substrate, which in principle is considered a generic property of the substrate. Now with the determined values of δ_i , J_{Ic} and $\int_0^{\delta_i} F dx$,

the BSI can be calculated accordingly for substrate with given geometry. Table 1 lists the details of each terms involved in the calculation of BSI from experimental data. Obviously, the value of BMG blade and MGTF coated blade (0.25 and 0.23, respectively) is smaller than that of commercial one (0.34), which equivalently being interpreted as 26.5% and 32% improvement on the sharpness.

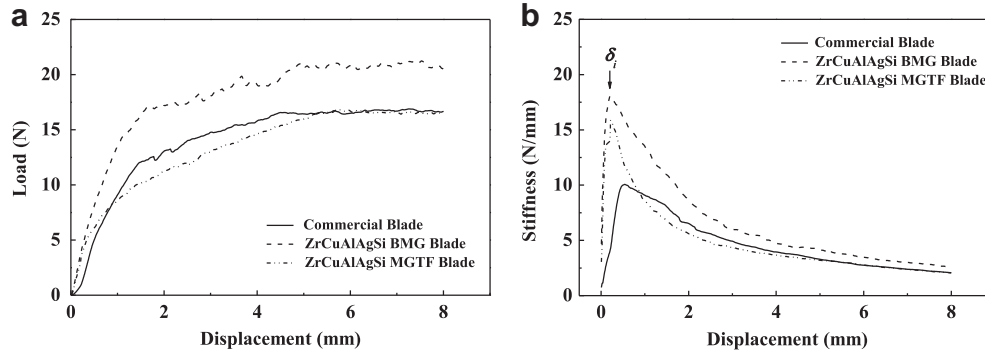


Fig. 7. (a) Load–displacement and (b) Stiffness–displacement curves of the first cutting pass for all three blades evaluated by indentation–cutting test.

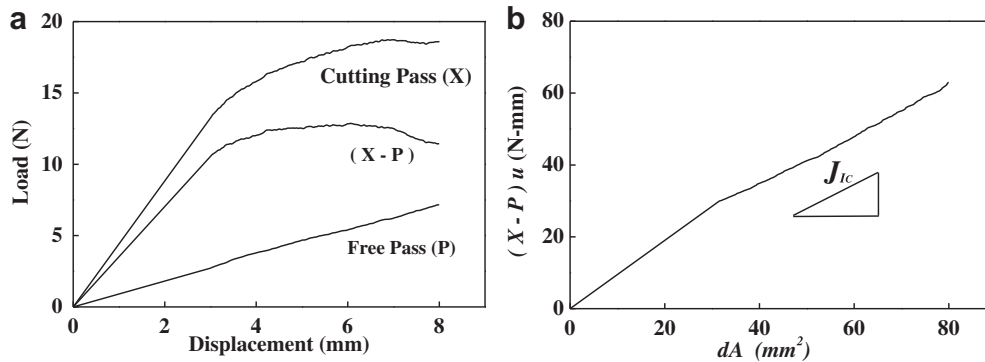


Fig. 8. Typical (a) Load–displacement curves of the 1st (X, cutting pass) and 2nd (P, free pass), at the same cutting position of substrate for the ZrCuAlAgSi MGTF coated blade; (b) $(X - P)u$ term as a function of cut area dA .

Table 1
Indicators of blade sharpness index (BSI) calculation.

	δ_i	E_i	J_{Ic}	BSI
Commercial blade	0.54	1.121	1.24	0.34
ZrCuAlAgSi MG blade	0.195	0.304	1.24	0.25
ZrCuAlAgSi MGTF blade	0.216	0.309	1.24	0.23

4. Conclusion

An amorphous ZrCuAlNiSi BMG blade was successfully fabricated from a ZrCuAlAgSi BMG plate by EDC and fine polish process. Both ZrCuAlAgSi BMG blade and ZrCuAlAgSi MGTF coated blade exhibits smoother surface and lower roughness than the commercial one. A customized sharpness test further reveals that the BSI value of BMG blade and MGTF coated blade (0.25 and 0.23, respectively) is smaller than that of the commercial blade (0.34). This provides a good quantitative confirmation on that both the BMG and MGTF coated blades have a better cutting ability than the commercial one. Both ZrCuAlAgSi BMG and MGTF coated blades are believed to be new options for cutting tools and can be used in medical applications.

Acknowledgment

The authors would like to grateful acknowledge the sponsorship from National Science Council of Taiwan, ROC under the Contract No. NSC 98-2221-E-008-116-MY3 and NSC100-2120-M-110-004. In

addition, the authors like to acknowledge the help on the scratch test and AFM analysis by Prof. S. I. Chang of National Chung Hsing University.

References

- [1] Inoue A. Acta Mater 2000;48:279.
- [2] Wang WH, Dong C, Shek CH. Mater Sci Eng R 2004;44:45; Schuh CA, Hufnagel TC, Ramamurty U. Acta Mater 2007;55:4067.
- [3] Yavari AR, Lewandowski JJ, Eckert J. MRS Bull 2007;32:635.
- [4] Chen MW. Annu Rev Mater Res 2008;38:14.1.
- [5] Huang JC, Chu JP, Jang JSC. Intermetallics 2009;17:973–87.
- [6] Inoue A, Takeuchi A. ActaMater 2011;59:2243.
- [7] Suryanarayana C, Inoue A. Bulk metallic glasses. FL, USA: CRC Press (Taylor & Francis Group; 2011.
- [8] Sharma P, Kaushik N, Kimura H, Saotome Y, Inoue A. Nanotechnology 2007; 18:035302.
- [9] Schroers J. Adv Mater 2010;22:1566.
- [10] Telford M. Mater Today 2004;7:36.
- [11] Chiang PT, J Chen G, Jian SR, Shih YH, Jang JSC, Lai CH. Fooyin J Health Sci 2010;2:12.
- [12] Chu CW, Jang Jason SC, Chiu SM, Chu JP. Thin Solid Films 2009;517:4930.
- [13] He W, Chuang A, Cao Z, Liaw PK. Metall Mater Trans A 2010;41:1726.
- [14] Schroers J, Kumar G, Hodges T, Chan S, Kyriakides T. JOM 2009;61:21.
- [15] Chu JP, Huang JC, Jang JSC, Wang YC, Liaw PK. JOM 2010;62:19.
- [16] Chu CW, Jang Jason SC, Chen GJ, Chiu SM. Surf Coat Tech 2008;202:5564.
- [17] Stepien Piotr. Wear 2010;269:249.
- [18] Black D, Marks R, Caunt A. Bioeng and Skin 1985;1:111–23.
- [19] Izmailov GA, Orenburov PI, Repin VA, Gorbunov SM, Ismailov SG. Khirurgiia (Mosk) 1989;6:75.
- [20] McCarthy CT, Hussey M, Gilchrist MD. Eng Fracture Mechanics 2007;74:2205.
- [21] McCarthy CT, Annaidh AN, Gilchrist MD. Eng Fracture Mechanics 2010;77: 437.